

Merging dynamical and structural indicators to measure resilience in multispecies systems

Lucas P. Medeiros^{1*}, Chuliang Song^{1*}, Serguei Saavedra^{1†}

¹Department of Civil and Environmental Engineering, MIT
77 Massachusetts Av., 02139 Cambridge, MA, USA

RUNNING TITLE: Merging dynamical and structural indicators of resilience

*Equal contribution

†To whom correspondence should be addressed. E-mail: sersaa@mit.edu ORCID 0000-0003-1768-363X

1 Summary

- 2 1. Resilience is broadly understood as the ability of an ecological system to resist and recover
3 from perturbations acting on species abundances and on the system's structure. However,
4 one of the main problems in assessing resilience is to understand the extent to which mea-
5 sures of recovery and resistance provide complementary information about a system. While
6 recovery from abundance perturbations has a strong tradition under the analysis of dynam-
7 ical stability, it is unclear whether this same formalism can be used to measure resistance
8 to structural perturbations (e.g., perturbations to model parameters).
- 9 2. Here, we provide a framework grounded on dynamical and structural stability in Lotka-
10 Volterra systems to link recovery from small perturbations on species abundances (i.e.,
11 dynamical indicators) with resistance to parameter perturbations of any magnitude (i.e.,
12 structural indicators). We use theoretical and experimental multispecies systems to show
13 that the faster the recovery from abundance perturbations, the higher the resistance to
14 parameter perturbations.
- 15 3. We first use theoretical systems to show that the return rate along the slowest direction
16 after a small random abundance perturbation (what we call full recovery) is negatively
17 correlated with the largest random parameter perturbation that a system can withstand
18 before losing any species (what we call full resistance). We also show that the return rate
19 along the second fastest direction after a small random abundance perturbation (what we
20 call partial recovery) is negatively correlated with the largest random parameter perturba-
21 tion that a system can withstand before at most one species survives (what we call partial
22 resistance). Then, we use a data set of experimental microbial systems to confirm our the-
23 oretical expectations and to demonstrate that full and partial components of resilience are
24 complementary.
- 25 4. Our findings reveal that we can obtain the same level of information about resilience by
26 measuring either a dynamical (i.e., recovery) or a structural (i.e., resistance) indicator. Ir-
27 respective of the chosen indicator (dynamical or structural), our results show that we can
28 obtain additional information by separating the indicator into its full and partial compo-
29 nents. We believe these results can motivate new theoretical approaches and empirical
30 analyzes to increase our understanding about risk in ecological systems.

31 KEYWORDS: dynamical stability, feasibility, microbial systems, recovery, resistance, species
32 composition, structural stability

33 Introduction

34 Ecological systems such as bird species competing for resources (Gibbs & Grant, 1987), plants
35 and their mutualistic pollinators (Burkle *et al.*, 2013), and microbes interacting in the human
36 gut (Costello *et al.*, 2012) face constant perturbations in changing environments. The *resilience*
37 of such systems to different types of perturbations has been one of the most debated concepts
38 in ecological research and has important implications for biodiversity and ecosystem functioning
39 (Hodgson *et al.*, 2015; Folke *et al.*, 2016; Pimm *et al.*, 2019). Broadly, resilience has been referred
40 to as the ability of an ecological system to resist and recover from external perturbations (Hodgson
41 *et al.*, 2015; Capdevila *et al.*, 2020). To understand these concepts and measures, epistemological
42 work has established three necessary conditions to study ecological responses to perturbations
43 (Justus, 2013): (i) a description of the ecological system, which mathematically takes the form
44 of a *population dynamics model*, (ii) the definition of a *reference state* from which the system
45 will be perturbed, and (iii) the definition of the type and magnitude of *perturbations*, which can
46 act on state variables, model parameters (i.e., the system's structure), or both (see Glossary).
47 Following this rationale, *recovery* (although it has also been called resilience, see Justus (2013)
48 and Pimm *et al.* (2019)) has been typically defined as how fast a system returns to a reference
49 state after a given perturbation (Hodgson *et al.*, 2015; Capdevila *et al.*, 2020). In turn, *resistance*
50 has been defined as how much change a system can exhibit after a given perturbation (Hodgson
51 *et al.*, 2015; Capdevila *et al.*, 2020). Hence, a sufficient condition for a system to be resilient is to
52 exhibit fast recovery and high resistance. However, in order to assess the resilience of a system,
53 it is paramount to have informative indicators of recovery and resistance and to understand the
54 interconnection between these two measures, which may not necessarily be complementary (i.e.,
55 provide different qualitative information about the resilience of a system) (Domínguez-García
56 *et al.*, 2019; Kéfi *et al.*, 2019).

57 Recovery has had a strong tradition in the mathematical analysis of *asymptotic dynamical stability*
58 (hereafter dynamical stability) (Strogatz, 2001). In ecology, recovery has been typically concep-
59 tualized as the return rate along the slowest direction to a reference equilibrium state (Pimm
60 & Lawton, 1977; Dakos *et al.*, 2015; Donohue *et al.*, 2016). This return rate can be quantified
61 by the real part of the largest eigenvalue (if negative) of the Jacobian matrix when evaluated at
62 equilibrium (Novak *et al.*, 2016; Logofet, 2018). The Jacobian matrix represents the linearized
63 dynamical forces acting around a given state. This implies that recovery has been mathematically
64 quantified by the long-term return rate (or the return time if inverted) of a system to a reference
65 equilibrium state after small perturbations (per the linear validity of the Jacobian) acting on
66 species abundances (i.e., the state variables of the system).

67 By contrast, the measurement of resistance has had a weaker tradition in the field of dynamical
68 systems (Strogatz, 2001) and it is unclear whether it can be linked to dynamical stability in
69 ecological systems (Justus, 2013; Domínguez-García *et al.*, 2019). Resistance has been typically
70 quantified as the magnitude of displacement of a system following a perturbation (Carpenter *et al.*,
71 1992; Hillebrand *et al.*, 2018). Differently from recovery, resistance is not necessarily limited to
72 a particular quantitative equilibrium state (i.e., abundance distribution at equilibrium), and it is
73 expected to reflect the response of a system to perturbations acting on both species abundances
74 and on the structure of a system (Donohue *et al.*, 2016; Pimm *et al.*, 2019). Formally, this
75 structure can be represented by a population dynamics model describing the governing laws of a
76 system and its parameters (Justus, 2013). That is, while species abundances represent the state
77 variables of a system, the structure represents the model parameters (and the model itself). Thus,
78 it remains unclear whether recovery from abundance perturbations and resistance to structural
79 perturbations can be quantified within the same formalism, and whether there are potential
80 connections between these two aspects of resilience (Hodgson *et al.*, 2015; Pimm *et al.*, 2019).

81 Focusing on parameter perturbations, a dynamical system is said to be *structurally stable* if the
82 topology of the phase portrait (i.e., the qualitative behavior of a dynamical system) is preserved
83 under smooth parameter changes (Smale, 1967; Arnold, 1988). For example, a system with S
84 species can be considered structurally stable if none of the species goes extinct after small changes
85 in the parameters corresponding to species intrinsic growth rates (Saavedra *et al.*, 2017). Import-
86 tantly, it has already been shown that the sensitivity to stochastic perturbations of abundances
87 in the vicinity of an equilibrium is equivalent to the sensitivity to fluctuations of the parameters
88 within the same vicinity (Arnoldi & Haegeman, 2016). Specifically, the response to external
89 infinitesimal perturbations acting on species abundances agrees with the minimal parameter per-
90 turbation able to render the system dynamically unstable. Furthermore, structurally unstable
91 systems (i.e., systems that change their qualitative behavior after small parameter changes) are
92 characterized by conditions under which the largest eigenvalue of the Jacobian matrix is equal to
93 zero (Strogatz, 2001; Duan, 2015). These previous results have established a potential direction to
94 link dynamical indicators (i.e., measures related to perturbations acting on species abundances)
95 with structural indicators (i.e., measures related to perturbations acting on model parameters) to
96 measure resilience in ecological systems (Dobrinevski & Frey, 2012; Constable & McKane, 2015;
97 Cenci & Saavedra, 2018).

98 Here, we extend the connection between dynamical and structural indicators beyond the vicinity
99 of an equilibrium state to study resilience in multispecies ecological systems. Specifically, we
100 link recovery with dynamical stability and define it as the long-term return rate of a system to

101 a quantitative reference state (i.e., abundance distribution at equilibrium) after small random
102 perturbations on species abundances. We then separate recovery into *full* and *partial recovery*
103 as to whether species abundances return fully or partially to such quantitative reference state,
104 respectively. Next, we link resistance with structural stability and define it as the ability of a
105 system to remain in a qualitative reference state (i.e., species composition at equilibrium) after
106 random parameter perturbations of any magnitude. We then separate resistance into *full* and
107 *partial resistance* as to whether all the species or at most one species remains in such qualitative
108 reference state, respectively. Therefore, we define *full resilience* as the capacity of a system to
109 maintain its full species composition through the recovery and resistance of all species. Then,
110 we define *partial resilience* as the capacity of a system to maintain a partial species composition
111 through the recovery and resistance of a subset of species (see Glossary).

112 We first illustrate our framework using theoretically parameterized ecological systems spanning
113 multiple interaction types and number of species. In particular, we explore competition, mutual-
114 istic, and antagonistic systems with 3, 4, and 5 species. Overall, we find that when considering
115 abundance and parameter perturbations together, recovery and resistance are interconnected
116 measures of resilience. However, we show that these dynamical and structural indicators can
117 provide complementary information about a system when separated into full and partial re-
118 siliance. Then, we apply our framework to 17 experimentally parameterized microbial systems
119 containing three interacting species each. We corroborate our theoretical results that full and
120 partial resilience are complementary components of experimental systems. Finally, we discuss
121 the implications of our findings and future avenues of research on resilience.

122 **Methods**

123 **Population dynamics model**

124 To study and measure resilience in ecological systems, it is necessary to define (i) a population
125 dynamics model, (ii) a reference state, and (iii) the system's response as a function of the type
126 and magnitude of perturbations (Justus, 2013). Focusing on the model, we assume that the
127 dynamics of ecological systems are governed by any model topologically equivalent to the classic
128 Lotka-Volterra (LV) dynamics. It has been shown that if the unstable and stable equilibria of
129 the classic LV model can be mapped into the unstable and stable equilibria of a modified model,
130 then this modified model is topologically equivalent to the classic LV (Cenci & Saavedra, 2018;

131 Saavedra *et al.*, 2020). The classic LV model written in the r-formalism is given by (Case, 2000):

$$\frac{dN_i}{dt} = N_i \left(r_i + \sum_{j=1}^S a_{ij} N_j \right), \quad i = 1, \dots, S \quad (1)$$

132 where N_i is the abundance (or biomass) of species i , S is the number of species in the system,
133 and a_{ij} is an element of the interaction matrix $\mathbf{A} = \{a_{ij}\}$ representing the per capita effect of
134 species j on species i . The phenomenological parameter r_i is the intrinsic growth rate of species i ,
135 representing how abiotic factors affect the balance between mortality and resource intake (Case,
136 2000; Coulson *et al.*, 2017).

137 To investigate resilience in the classic LV model, we generate fully connected random interaction
138 matrices \mathbf{A} by setting the diagonal elements to $a_{ii} = -1 \forall i$ (introducing the biological principle of
139 self-regulation), whereas the off-diagonal elements a_{ij} ($i \neq j$) are randomly drawn from a normal
140 distribution with mean zero and variance σ^2 (i.e., $a_{ij} \sim \mathcal{N}(0, \sigma^2)$). Note that the value of σ^2 sets
141 the relative strength of interspecific interactions (a_{ij}) given that intraspecific interactions are fixed
142 (i.e., $a_{ii} = -1$). To explore different types of ecological systems, we introduce sign constraints:
143 (i) $a_{ij} < 0$ for competition systems, (ii) $a_{ij} > 0$ for mutualistic systems, and (iii) $a_{ij}a_{ji} < 0$ for
144 antagonistic systems (Murdoch *et al.*, 2003; Allesina & Tang, 2012) (see *Resilience in theoretical*
145 *systems*). Applying these constraints is equivalent to sampling a_{ij} from a half-normal distribution
146 and taking the appropriate sign reversal (Allesina & Tang, 2012; Song *et al.*, 2020). For simplicity,
147 we only explore one type of antagonistic network structure given by a matrix \mathbf{A} where $a_{ij} < 0$ if
148 $i > j$ and $a_{ij} > 0$ if $i < j$ (e.g., a trophic chain with omnivory). Note that, in these antagonistic
149 systems, the feasibility condition itself (i.e., $N_i^* > 0 \forall i$; see *Reference state*) constraints the r_i
150 values to be ecologically realistic as top predators and producers would necessarily have negative
151 and positive r_i values, respectively.

152 To guarantee that reference equilibrium states are dynamically stable (see *Reference state*), we
153 follow a probabilistic criteria for random matrices and set the variance of the distribution of
154 interaction strengths proportional to system size ($\sigma^2 = \frac{1}{S^2}$) (May, 1972). Note that having σ^2
155 to scale with the number of species S is an ecologically realistic assumption (Dougoud *et al.*,
156 2018). We also tested a scenario in which interspecific interactions are stronger (i.e., $\sigma^2 = \frac{1}{S}$) and
157 obtained similar results (Figures S3 and S4). It is important to note that, under our framework,
158 we cannot increase the relative strength of interspecific interactions beyond a certain limit in
159 order to guarantee dynamical stability. Thus, we assume that every species in our theoretical
160 systems (see *Resilience in theoretical systems*) is self-regulated, including predators in antagonistic
161 systems (Barabás *et al.*, 2017; Song & Saavedra, 2020).

162 Reference state

163 We consider a feasible and dynamically stable equilibrium as our reference state (Song & Saave-
164 dra, 2018; Song *et al.*, 2020). Feasibility corresponds to the capacity of a system to sustain all its
165 constituent species over the long-run. Formally, feasibility implies the existence of a positive so-
166 lution (i.e., $N_i^* > 0 \forall i$ under the equilibrium $dN_i/dt = 0$ in Equation (1)). Note that feasibility is
167 a necessary condition for persistence, permanence, and the existence of bounded orbits (Hofbauer
168 & Sigmund, 1998). In turn, we define dynamical stability as the capacity of a system to return
169 to its feasible equilibrium state after small random perturbations on species abundances. This is
170 fulfilled when all the eigenvalues of the Jacobian matrix (\mathbf{J}) when evaluated at the equilibrium
171 state ($\mathbf{N}^* = [N_1^*, \dots, N_S^*]^\top$, as defined by $d\mathbf{N}^*/dt = 0$) have negative real parts (May, 1972; Case,
172 2000).

173 For the classic LV dynamics (Equation (1)), the Jacobian matrix at a feasible equilibrium is
174 defined as:

$$\mathbf{J} = \text{diag}(\mathbf{N}^*) \cdot \mathbf{A}, \quad (2)$$

175 where $\text{diag}(\mathbf{N}^*)$ is a diagonal matrix with N_1^*, \dots, N_S^* in its diagonal. The equilibrium of the
176 classic LV model is given by the vector of species abundances $\mathbf{N}^* = -\mathbf{A}^{-1}\mathbf{r}$. This definition of
177 reference state has the advantage of allowing us to represent it as a quantitative or qualitative
178 reference state. Quantitatively, the focus is on the exact values of the feasible and dynamically
179 stable equilibrium \mathbf{N}^* (i.e., the species abundance distribution at equilibrium). Qualitatively, the
180 focus is on the existence of such a feasible equilibrium ($N_i^* > 0 \forall i$) (i.e., the species composition
181 at equilibrium).

182 Recovery from abundance perturbations

183 Regarding the response of a system to abundance perturbations, we focus on the standard defi-
184 nition of recovery linked to dynamical stability (Strogatz, 2001). Specifically, we define recovery
185 as the return rate of a system to a feasible and dynamically stable reference state after a small
186 perturbation on abundances. Formally, we use as indicators the real part of the largest (λ_1) and
187 second smallest (λ_{S-1}) eigenvalues of the Jacobian matrix (\mathbf{J}) evaluated at equilibrium (Equation
188 (2)). The largest eigenvalue (if negative) measures the return rate along the slowest direction
189 of recovery. Because species abundances will have recovered completely after going through the
190 slowest direction, we use λ_1 as an indicator of full recovery. The second smallest eigenvalue (if
191 negative) represents the return rate along the second fastest direction. Because species abun-
192 dances will have only partially recovered after going through the second fastest direction, we

193 use λ_{S-1} as an indicator of partial recovery. Thus, for each possible feasible and dynamically
 194 stable state (\mathbf{N}^*) of a system, we use λ_1 and λ_{S-1} as a measure of its full and partial recovery,
 195 respectively (Figures 1a and 1b). To be able to compare λ_1 and λ_{S-1} across different equilibrium
 196 states, we normalize \mathbf{N}^* to unit norm (i.e., $\frac{\mathbf{N}^*}{\|\mathbf{N}^*\|}$) before computing these indicators.

197 Resistance to parameter perturbations

198 Shifting our focus to the response of a system to random parameter perturbations of any mag-
 199 nitude, we base our analysis on the concept of structural stability and link it with resistance.
 200 We define resistance as the smallest random parameter perturbation that a system can tolerate
 201 without affecting its qualitative reference state (defined as a feasible and dynamically stable equi-
 202 librium). For a given interaction matrix \mathbf{A} , feasibility in the classic LV model will be satisfied
 203 as long as the \mathbf{r} -vector falls inside the feasibility domain defined as (Song *et al.*, 2018; Medeiros
 204 *et al.*, 2020):

$$D_F(\mathbf{A}) = \{ \mathbf{r} \in \mathbb{R}^S \mid \mathbf{r} = N_1^* \mathbf{v}_1 + \dots + N_S^* \mathbf{v}_S, \text{ with } N_1^*, \dots, N_S^* > 0 \}, \quad (3)$$

205 where $-\mathbf{v}_i$ is the i th column vector of \mathbf{A} and N_i^* is the feasible (i.e., positive) abundance of species
 206 i at equilibrium. Geometrically, $D_F(\mathbf{A})$ is a cone in S dimensions and any \mathbf{r} -vector inside the
 207 cone gives rise to a feasible solution. Note that only the direction of the \mathbf{r} -vector matters because
 208 if Equation (3) is satisfied for a given vector \mathbf{r} , it is also satisfied for a scaled vector $c\mathbf{r} \forall c > 0$.
 209 Therefore, the region inside the borders of $D_F(\mathbf{A})$ corresponds to the specific directions of \mathbf{r} for
 210 which the system is feasible (Saavedra *et al.*, 2017). Ecologically, this domain defines the range
 211 of conditions linked to abiotic factors, which are phenomenologically represented by the direction
 212 of the \mathbf{r} -vector, compatible with the persistence of all species in the system characterized by \mathbf{A}
 213 (Song *et al.*, 2020; Medeiros *et al.*, 2020). Note that we do not impose any restriction on the sign
 214 of the elements r_i of the \mathbf{r} -vector, they can be positive or negative depending on $D_F(\mathbf{A})$ (Song
 215 *et al.*, 2018).

216 Importantly, starting from a feasible equilibrium state \mathbf{N}^* , a border of $D_F(\mathbf{A})$ (i.e., $\mathbf{r} = \sum_{i=1}^S N_i^* \mathbf{v}_i$
 217 with $N_j^* = 0$ and $N_i^* > 0 \forall i \neq j$) represents a limit in the direction of \mathbf{r} where at least one
 218 of the S species (i.e., species j) goes extinct (Rohr *et al.*, 2016; Grilli *et al.*, 2017; Tabi *et al.*,
 219 2020). Similarly, a vertex of $D_F(\mathbf{A})$ (i.e., $\mathbf{r} = N_i^* \mathbf{v}_i$, with $N_i^* > 0$ and $N_j^* = 0 \forall j \neq i$) represents
 220 a limit in the direction of \mathbf{r} where a single species (i.e., species i) survives at most, depending
 221 on whether this species is self-sustained (Rohr *et al.*, 2016; Grilli *et al.*, 2017; Tabi *et al.*, 2020).
 222 For example, with three species, if one sets $N_1^* = 0$, the \mathbf{r} -vector will lie on one of the borders

223 of the cone ($D_F(\mathbf{A})$), which is given by $\mathbf{r} = N_2^* \mathbf{v}_2 + N_3^* \mathbf{v}_3$, with $N_2^*, N_3^* > 0$. Furthermore, if
 224 $N_1^* = 0$ and $N_2^* = 0$, then the \mathbf{r} -vector will lie on one of the vertices of $D_F(\mathbf{A})$, which is given by
 225 $\mathbf{r} = N_3^* \mathbf{v}_3$, with $N_3^* > 0$. Thus, we focus on the shortest distances that a system can withstand
 226 before hitting a border or vertex under random perturbations to \mathbf{r} . Note that we focus on random
 227 perturbations as we typically have no a priori information about the direction of environmen-
 228 tal perturbations. Importantly, measuring such distances in the parameter space allows us to
 229 consider how resistant a system is to parameter perturbations of any magnitude.

230 Because it is only necessary to know the direction (not the magnitude) of \mathbf{r} to know if a system
 231 \mathbf{A} is feasible, we normalize the intrinsic growth rates to unit norm (i.e., $\frac{\mathbf{r}}{\|\mathbf{r}\|}$). Then, the distance
 232 between an intrinsic growth rate vector inside the feasibility domain ($\mathbf{r}(\mathbf{N}^*)$) and a border of
 233 $D_F(\mathbf{A})$ can be calculated by the arc length (i.e., angle) between $\mathbf{r}(\mathbf{N}^*)$ and $\mathbf{r}(\text{border})$ as: $d_b =$
 234 $\arccos(\mathbf{r}(\mathbf{N}^*) \cdot \mathbf{r}(\text{border}))$, where $\mathbf{r}(\text{border})$ is the orthogonal projection of $\mathbf{r}(\mathbf{N}^*)$ onto the border
 235 (Grilli *et al.*, 2017). For a system with S species, each $\mathbf{r}(\mathbf{N}^*)$ inside the feasibility domain is
 236 associated with one distance to each of the $\binom{S}{S-1} = S$ borders. We focus on the distance to
 237 the closest border ($\min\{d_b\}$). Thus, the distance of a system to the closest border ($\min\{d_b\}$)
 238 represents the largest random parameter perturbation that the system can withstand before
 239 losing any species—which we call full resistance. Similarly, the distance between $\mathbf{r}(\mathbf{N}^*)$ and a
 240 vertex of $D_F(\mathbf{A})$ can be calculated by the arc length between $\mathbf{r}(\mathbf{N}^*)$ and $\mathbf{r}(\text{vertex})$ as: $d_v =$
 241 $\arccos(\mathbf{r}(\mathbf{N}^*) \cdot \mathbf{r}(\text{vertex}))$, where $\mathbf{r}(\text{vertex})$ is the \mathbf{r} -vector associated with the vertex. Note that
 242 the \mathbf{r} -vector associated with a given vertex is equal to the corresponding column vector of \mathbf{A} scaled
 243 by the single species abundance at equilibrium (i.e., $\mathbf{r} = N_i^* \mathbf{v}_i$). For a system with S species,
 244 each $\mathbf{r}(\mathbf{N}^*)$ inside the feasibility domain is associated with one distance to each of the $\binom{S}{1} = S$
 245 vertices. We focus on the distance to the closest vertex ($\min\{d_v\}$). Therefore, the distance of
 246 a system to the closest vertex ($\min\{d_v\}$) represents the largest random parameter perturbation
 247 that a system can withstand before it is reduced to at most a single species—which we call partial
 248 resistance (Figures 1c and 1d).

249 Resilience in theoretical ecological systems

250 First, we investigate the potential associations between recovery and resistance according to our
 251 measures described above across several theoretical systems (i.e., matrices \mathbf{A}). To do so, we
 252 first generate three types of random matrices: competition systems, mutualistic systems, and
 253 antagonistic systems (see *Population dynamics model*). For each of these three types of system,
 254 we generate 100 random matrices \mathbf{A} by sampling the interspecific interaction coefficients a_{ij} from
 255 $\mathcal{N}(0, \frac{1}{S^2})$ for three different system sizes: $S = 3, 4$, and 5 species. Then, for each random matrix,

256 we sample $100 \times 2^{(S-2)}$ feasible equilibria (i.e., $\mathbf{N}^* > 0$) uniformly on the unit S -dimensional
257 hypersphere (i.e., $\|\mathbf{N}^*\| = 1$) and solve for the intrinsic growth rates: $\mathbf{r} = -\mathbf{A}\mathbf{N}^*$. To guarantee
258 dynamical stability in addition to feasibility, we only sample equilibrium states for which the
259 real part of the largest eigenvalue of $\mathbf{J} = \text{diag}(\mathbf{N}^*)\mathbf{A}$ is negative. We eliminate random matrices
260 for which all sampled equilibrium states had a non-negative largest eigenvalue. Note that we
261 increase the number of sampled equilibrium states exponentially with S to account for the fact
262 that sparsity among points grows exponentially with the number of dimensions.

263 For each feasible and dynamically stable equilibrium state that we sample, we calculate its full re-
264 covery (largest eigenvalue, λ_1), partial recovery (second smallest eigenvalue, λ_{S-1}), full resistance
265 (distance to closest border, $\min\{d_b\}$), and partial resistance (distance to closest vertex, $\min\{d_v\}$).
266 To investigate whether recovery and resistance are linked, we compute the Pearson correlation
267 coefficient (hereafter correlation) between full recovery and full resistance ($\rho(\lambda_1, \min\{d_b\})$), as
268 well as the correlation between partial recovery and partial resistance ($\rho(\lambda_{S-1}, \min\{d_v\})$). We
269 compute such correlations separately for each random system \mathbf{A} . A strong negative correlation
270 indicates that the faster the recovery from abundance perturbations, the higher the resistance to
271 parameter perturbations (Figure 1). Finally, we study the complementarity between our indi-
272 cators by computing the partial correlation between λ_1 and λ_{S-1} controlling for the rank of λ_1
273 ($\rho(\lambda_1, \lambda_{S-1} \mid \text{rank of } \lambda_1)$). This control is necessary to account for the fact that $\lambda_1 \geq \lambda_{S-1}$ for each
274 equilibrium state by definition. We also compute the partial correlation between $\min\{d_b\}$ and
275 $\min\{d_v\}$ controlling for the rank of $\min\{d_v\}$ ($\rho(\min\{d_b\}, \min\{d_v\} \mid \text{rank of } \min\{d_v\})$). Note that
276 $\min\{d_v\} \geq \min\{d_b\}$ for each equilibrium state. A value close to zero of these partial correlations
277 would imply the that full and partial components are complementary.

278 Resilience in experimental microbial systems

279 Next, we investigate the complementarity and potential application of our indicators of resilience
280 using experimental ecological systems. For this purpose, we use 17 feasible and dynamically stable
281 systems where each system consists of three interacting soil-dwelling bacteria species (Friedman
282 *et al.*, 2017). These publicly available data come from a very detailed and controlled study
283 performing persistence experiments by co-inoculating different combinations of heterotrophic soil-
284 dwelling bacteria species at varying initial fractions and propagating them through five growth-
285 dilution cycles (Friedman *et al.*, 2017). Each 3-species experimental system is characterized by
286 an interaction matrix \mathbf{A} and an intrinsic growth rate vector \mathbf{r} . The experimental values of \mathbf{r} were
287 inferred by fitting via least-squares the classic LV model (Equation (1)) to the observed abundance
288 time series of species monocultures (Friedman *et al.*, 2017) (Table S1). Each interaction matrix

289 \mathbf{A} was inferred through pairwise tournaments by fitting via least-squares Equation (1) to the
290 observed time series of species abundances (Friedman *et al.*, 2017) (Table S2). Although more
291 than 17 systems with three species are available from this data set, we only use the systems for
292 which the equilibrium state obtained using the experimentally inferred matrix \mathbf{A} and intrinsic
293 growth rate vector \mathbf{r} ($\mathbf{N}^* = -\mathbf{A}^{-1}\mathbf{r}$) is feasible and dynamically stable (Table S3).

294 Importantly, interaction matrices contained competition interactions (i.e., $a_{ij}, a_{ji} < 0$), antag-
295 onistic interactions (i.e., $a_{ij} < 0, a_{ji} > 0$), or a mix of both. It is also important to note that
296 the strength of inferred interactions (a_{ij}) varies greatly across and within experimental systems
297 (Table S2), allowing us to test our framework for different scenarios of interaction strengths. For
298 each of the 17 systems (each combination of \mathbf{A} and \mathbf{r}), we calculate its full and partial resilience
299 components following the same methodology as described above (see *Resilience in theoretical*
300 *systems*). Additionally, for each experimental system, we randomly sampled 2,000 feasible and
301 dynamically stable equilibria uniformly on the positive orthant of the unit sphere (i.e., $\mathbf{N}^* > 0$,
302 $\|\mathbf{N}^*\| = 1$, and $\lambda_1 < 0$) and measured our resilience indicators for each one of these sampled
303 equilibria. The rationale behind sampling these 2,000 random equilibria was to compare the
304 full/partial recovery and full/partial resistance observed for the experimental systems with other
305 potential values of these indicators that could have been observed under different conditions.

306 Following our analysis with theoretical systems, for each of the 17 experimental systems, we study
307 the complementarity of our indicators by computing the partial correlation between full recovery
308 and partial recovery (λ_1, λ_2) controlling for the rank of λ_1 ($\rho(\lambda_1, \lambda_2 \mid \text{rank of } \lambda_1)$) as well as the
309 partial correlation between full resistance and partial resistance ($\min\{d_b\}, \min\{d_v\}$) controlling
310 for the rank of $\min\{d_v\}$ ($\rho(\min\{d_b\}, \min\{d_v\} \mid \text{rank of } \min\{d_v\})$). Then, in order to properly
311 summarize the relationship between full and partial resilience across systems, we compute a
312 relative value for each indicator ($\tilde{\lambda}_1, \tilde{\lambda}_2, \min\{\tilde{d}_b\}$, and $\min\{\tilde{d}_v\}$) by dividing each indicator by
313 its minimum (recovery indicators) or maximum (resistance indicators) possible value that can be
314 attained inside its corresponding feasibility domain. For example, the relative value of λ_1 ($\tilde{\lambda}_1$) for
315 a given experimental equilibrium state \mathbf{N}^* is obtained by dividing λ_1 by the minimum value of λ_1
316 attained over all 2,000 randomly sampled equilibria \mathbf{N}^* , i.e., $\tilde{\lambda}_1 = \frac{\lambda_1}{\min\{\lambda_1\}}$. Thus, relative values
317 close to zero or one represent systems that have the minimum or maximum possible resilience,
318 respectively. It is worth highlighting that this normalization does not allow us (and it is not
319 intended) to compare the level of resilience between two different systems, only their resilience
320 relative to the maximum possible value within the feasibility domain of the given system. Thus,
321 a large variation in the experimental values of relative full and partial resilience can indicate a
322 strong heterogeneity of resilience patterns across systems.

Results

We found that fast recovery from abundance perturbations (i.e., state variables, N_i^*) is associated with a high resistance to parameter perturbations (i.e., perturbations on intrinsic growth rates, r_i). Specifically, we found a strong negative correlation between full recovery (largest eigenvalue, λ_1) and full resistance (distance to closest border, $\min\{d_b\}$) across the three types of theoretical ecological systems (competition, mutualistic, and antagonistic systems; Figures 2a, S1, and S2). Moreover, we found that this strong association between full recovery and full resistance holds for multiple random systems with different number of species (Figure 2b, Table S4). We obtained similar results for stronger interspecific interactions (i.e., $\sigma^2 = \frac{1}{S}$), but correlations can be weaker due to a smaller variation in λ_1 and highly asymmetric feasibility domains (i.e., high variation among the border lengths) (Figure S3). We can understand this result by noting that the Jacobian matrix associated with an \mathbf{r} -vector on a border of the feasibility domain will have a row of zeros, which implies that the largest eigenvalue of this matrix will be zero (Figure 1a). In particular, all elements of the i th row of the Jacobian will be zero when the system is located at the border where $N_i^* = 0$. Recall that all eigenvalues of the Jacobian matrix need to be negative in order to guarantee dynamical stability and more negative values imply faster recovery.

Similarly, we found a strong negative correlation between partial recovery (second smallest eigenvalue, λ_{S-1}) and partial resistance (distance to closest vertex, $\min\{d_v\}$) across the three types of theoretical systems (Figure 3a, S1, and S2). In addition, we confirmed that this strong relationship between partial recovery and partial resistance holds for multiple random systems with different number of species (Figure 3b, Table S4), even when interspecific interactions are stronger (Figure S4). Similarly to the association between λ_1 and $\min\{d_b\}$, the association between λ_{S-1} and $\min\{d_v\}$ can be understood by noting that the Jacobian matrix associated with an \mathbf{r} -vector on a vertex will have $S - 1$ rows of zeros. This implies that the largest $S - 1$ eigenvalues of the Jacobian will be zero at a vertex and, therefore, the second smallest eigenvalue will be associated with the distance to the closest vertex (Figures 1a and 1b).

We can additionally separate the relationship between recovery (full or partial) and resistance (full or partial) by the different vertices of the feasibility domain, noting that each vertex corresponds to the dominant species in the system (represented by different symbols in Figures 2a and 3a) (Rohr *et al.*, 2016; Tabi *et al.*, 2020). The extent to which the relationship between recovery and resistance may differ across vertices depends on the level of asymmetry in the feasibility domain (Rohr *et al.*, 2016; Tabi *et al.*, 2020). However, regardless of the asymmetry in the feasibility domain or the identity of the most abundant species, the relationship between recovery and

356 resistance remains strongly negative for each vertex (Figures 2a and 3a). To further explore this
357 result, we computed the partial correlation between recovery and resistance while controlling for
358 the identity of the most abundant species and, as expected, obtained slightly stronger correlation
359 values for λ_{S-1} and $\min\{d_v\}$ but not for λ_1 and $\min\{d_b\}$ (Figures S5 and S6; Table S5). In
360 addition, we also confirmed that our indicators of recovery (λ_1 and λ_{S-1}) and resistance ($\min\{d_b\}$
361 and $\min\{d_v\}$) are weakly correlated after controlling for the rank of the largest variable and,
362 therefore, complement each other (Figures S7 and S8; Table S5).

363 Moving to the experimental data, we confirmed the negative correlation between full recovery
364 (λ_1) and full resistance ($\min\{d_b\}$) (Figure 4a) as well as between partial recovery (λ_2) and partial
365 resistance ($\min\{d_v\}$) (Figure 4b) using 3-species microbial systems. In particular, we found
366 that $\rho(\lambda_1, \min\{d_b\})$ and $\rho(\lambda_2, \min\{d_v\})$ are strong and negative for all 17 experimental systems
367 (Figure 4c; Tables S6 and S7). Thus, the interconnections between recovery and resistance
368 remained strong for the experimental systems despite large differences in the type of interactions
369 (i.e., competition, antagonistic, or both interaction types) and interaction strengths (Figures S9
370 and S10).

371 Finally, we also confirmed that full resilience and partial resilience are complementary components
372 in the experimental data. Specifically, we found that all partial correlations between recovery
373 indicators (λ_1 and λ_2) and resistance indicators ($\min\{d_b\}$ and $\min\{d_v\}$) after controlling for
374 the rank of the largest variable were weak in the experimental systems (Figures 4c, 5a, and 5b).
375 Furthermore, this complementarity was also observed in the diversity of combinations between full
376 and partial resilience across systems. That is, while some systems appear to exhibit high relative
377 full resilience and high relative partial resilience (i.e., relative values close to 1), others appear to
378 exhibit low relative values (i.e., relative values close to 0; Figures 5c and 5d). In addition, some
379 systems appear to exhibit an asymmetry between the indicators—i.e., high relative full resilience
380 and low relative partial resilience and vice versa (Figures 5c and 5d). Note that correlations
381 between full recovery and full resistance ($\rho(\lambda_1, \min\{d_b\})$) as well as between partial recovery and
382 partial resistance ($\rho(\lambda_2, \min\{d_v\})$) are strong and negative, but not perfectly correlated (Figure
383 4c). Therefore, we should expect a strong qualitative mapping, but not a perfect quantitative
384 match between the position of a system in Figure 5c and its position in Figure 5d. This is
385 confirmed by strong and positive correlations between relative full recovery and relative full
386 resistance ($\rho(\tilde{\lambda}_1, \min\{\tilde{d}_b\}) = 0.83$) as well as between relative partial recovery and relative partial
387 resistance ($\rho(\tilde{\lambda}_2, \min\{\tilde{d}_v\}) = 0.64$). In sum, our results reveal that a wide diversity of relationships
388 between full and partial resilience is possible across ecological systems.

389 Discussion

390 The resilience of ecological systems to perturbations is one of the most important yet broadly
391 defined concepts in ecology and sustainability science (Hodgson *et al.*, 2015; Folke *et al.*, 2016;
392 Pimm *et al.*, 2019). Recently, the definition of resilience in ecology has been converging to the
393 capacity of an ecological system to resist and recover from external perturbations (Hodgson *et al.*,
394 2015; Capdevila *et al.*, 2020). However, there are still many open questions about how to measure
395 the response of multispecies systems to different types of perturbation, and the extent to which
396 these responses provide complementary information (Donohue *et al.*, 2016; Domínguez-García
397 *et al.*, 2019; Kéfi *et al.*, 2019). Understanding the different components of resilience and their
398 interconnections with respect to different types of perturbation is paramount to implement risk
399 assessment and conservation strategies in ecological systems (Folke *et al.*, 2004, 2016).

400 Here, we have introduced a new perspective in order to expand the way we measure resilience and
401 understand the connections among its components in three major ways. First, by acknowledging
402 that external perturbations can be of any type (i.e., abundance or parameter perturbations), we
403 have extended and integrated dynamical (i.e., focused on abundance perturbations) and struc-
404 tural (i.e., focused on parameter perturbations) indicators of resilience (Arnoldi & Haegeman,
405 2016; Saavedra *et al.*, 2017; Cenci & Saavedra, 2018). Specifically, we have found a clear link
406 between a dynamical stability indicator (long-term return rate of a system to a dynamically
407 stable equilibrium after small abundance perturbations) and a structural stability indicator (the
408 largest random parameter perturbation that a system can withstand before losing species). Thus,
409 differently from previous studies that have analyzed the associations between several resilience
410 indicators (Hillebrand *et al.*, 2018; Domínguez-García *et al.*, 2019), here we have focused only on
411 recovery and resistance and suggest a fundamental mathematical link between them when the
412 dynamics follows the LV model. This suggests that other potential mathematical links may ex-
413 ist between frequently used dynamical and structural indicators of resilience (Domínguez-García
414 *et al.*, 2019; Arnoldi *et al.*, 2016).

415 Second, we have found that recovery and resistance are interconnected when focusing on either
416 full or partial components. We have defined full resilience as the capacity of a system to maintain
417 its full species composition through the recovery and resistance of all species. In turn, we have
418 defined partial resilience as the capacity of a system to maintain a partial species composition
419 through the recovery and resistance of a subset of species. Specifically, we have shown that, under
420 the LV model, fast (full or partial) recovery from abundance perturbations implies a high (full
421 or partial) resistance to parameter perturbations. Therefore, we hypothesize that other hidden

422 connections between resilience indicators may be found if analyzed through the lens of full and
423 partial components (Kéfi *et al.*, 2019). From a practical point of view, this connection between
424 recovery and resistance means that we can monitor both of these aspects of resilience using a
425 small number of indicators (e.g., the eigenvalues of the Jacobian matrix of a system).

426 Third, we have found that full and partial resilience (either recovery or resistance) can be treated
427 as complementary components. Thus, our study proposes a novel way to understand orthogo-
428 nal dimensions of ecological resilience (Hillebrand *et al.*, 2018; Domínguez-García *et al.*, 2019).
429 Interestingly, full resilience is related to individual risk, whereas partial resilience is related to
430 systemic risk, two important concepts in ecological, financial, and other complex systems (Levin,
431 1998; Beale *et al.*, 2011). In fact, because full and partial resilience are complementary, focusing
432 on only one of these components may provide a misleading risk assessment of ecological systems
433 (Beale *et al.*, 2011). For example, our results show that a system that minimizes systemic risk
434 (i.e., is located as far as possible from the vertices of the feasibility domain) may still have a
435 high risk of losing individual species (i.e., is located close to a border of the feasibility domain;
436 Figures 1c and 1d). In particular, the existence of a wide diversity of relationships between full
437 and partial resilience in the studied experimental microbial systems suggests that future work
438 may investigate the extent to which these systems may be more exposed to individual or systemic
439 risk in the face of perturbations.

440 Our theoretical results can in principle be validated by performing perturbation experiments
441 with simple experimental systems (e.g., microbial systems). For instance, one can measure the
442 recovery rate of a system after small abundance perturbations (e.g., a single removal/addition
443 of individuals/biomass (Steiner *et al.*, 2006)) and the resistance to extinctions after structural
444 perturbations (e.g., a fixed change in temperature (Tabi *et al.*, 2020) or resource availability
445 (Hoek *et al.*, 2016)) over a set of baseline environmental conditions. Then, one can measure the
446 association between dynamical and structural indicators, that is, recovery rate and resistance to
447 extinctions. Furthermore, both indicators can be divided into their full (e.g., abundances fully
448 recover, no single-species extinctions) and partial (e.g., abundances partially recover, no systemic
449 collapse) components. For a given system, our theory purports an association between full (par-
450 tial) recovery and full (partial) resistance (Figures 4a and 4b), and no particular association
451 between full and partial components (recovery or resistance; Figures 5a and 5b).

452 Finally, it is worth mentioning that our indicators of resilience are formally derived under the
453 assumptions of feasible and dynamically stable equilibria with the classic LV model (Case, 2000).
454 Thus, these assumptions have to be fulfilled in order to apply our framework using empirical data.

455 Nevertheless, multiple methods have been developed to estimate the structure of nonequilibrium
456 systems (e.g., Jacobian matrix) without assuming a parameterized population dynamics model
457 (i.e., a nonparametric approach) (Ives *et al.*, 2003; Deyle *et al.*, 2016; Ushio *et al.*, 2018). In partic-
458 ular, previous work has shown that the divergence of a nonequilibrium vector field (characterized
459 by the trace of the Jacobian matrix) is associated with the extent to which the trajectory of the
460 system changes after parameter perturbations (Cenci & Saavedra, 2019; Cenci *et al.*, 2020)—a
461 measure of resistance. Thus, these previous results indicate that it may be possible to merge
462 concepts from dynamical and structural stability also under a nonparametric approach. In this
463 sense, we believe that our study may also add to the unification of parametric and nonparametric
464 approaches (Song & Saavedra, 2020) and could be expanded to be used with different types of
465 empirical data.

466 **Acknowledgments** Funding to SS was provided by NSF grant No. DEB-2024349.

467 **Competing financial interests** The authors declare no competing financial interests.

468 **Author contributions** All authors designed the study. LPM and CS performed the analysis.

469 SS supervised the study. All authors wrote the manuscript.

470 **Data accessibility** The R code and data supporting the results are archived at [https://doi.](https://doi.org/10.5281/zenodo.4390874)

471 [org/10.5281/zenodo.4390874](https://doi.org/10.5281/zenodo.4390874).

Accepted Article

472 References

- 473 Allesina, S. & Tang, S. (2012) Stability criteria for complex ecosystems. *Nature* **483**, 205–208.
- 474 Arnold, V.I. (1988) *Geometrical Methods in the Theory of Ordinary Differential Equations 2nd.*
475 Springer.
- 476 Arnoldi, J.F. & Haegeman, B. (2016) Unifying dynamical and structural stability of equilibria.
477 *Proc. of the Roy. Soc. London A: Mathematical, Physical and Engineering Sciences* **472**, 0874.
- 478 Arnoldi, J.F., Loreau, M. & Haegeman, B. (2016) Resilience, reactivity and variability: A mathe-
479 matical comparison of ecological stability measures. *Journal of Theoretical Biology* **389**, 47–59.
- 480 Barabás, G., Michalska-Smith, M.J. & Allesina, S. (2017) Self-regulation and the stability of large
481 ecological networks. *Nature Ecology and Evolution* **1**, 1870–1875.
- 482 Beale, N., Rand, D.G., Battey, H., Croxson, K., May, R.M. & Nowak, M.A. (2011) Individual
483 versus systemic risk and the regulator’s dilemma. *Proceedings of the National Academy of*
484 *Sciences* **108**, 12647–12652.
- 485 Burkle, L.A., Marlin, J.C. & Knight, T.M. (2013) Plant-pollinator interactions over 120 years:
486 loss of species, co-occurrence, and function. *Science* **339**, 1611–1615.
- 487 Capdevila, P., Stott, I., Beger, M. & Salguero-Gómez, R. (2020) Towards a comparative frame-
488 work of demographic resilience. *Trends in Ecology and Evolution* .
- 489 Carpenter, S.R., Kraft, C.E., Wright, R., He, X., Soranno, P.A. & Hodgson, J.R. (1992) Resilience
490 and resistance of a lake phosphorus cycle before and after food web manipulation. *The American*
491 *Naturalist* **140**, 781–798.
- 492 Case, T. (2000) *An Illustrated Guide to Theoretical Ecology*. Oxford University Press, Oxford.
- 493 Cenci, S., Medeiros, L.P., Sugihara, G. & Saavedra., S. (2020) Assessing the predictability of
494 nonlinear dynamics under smooth parameter changes. *Journal of the Royal Society Interface*
495 **17**, 20190627.
- 496 Cenci, S. & Saavedra, S. (2018) Structural stability of nonlinear population dynamics. *Physical*
497 *Review E* **97**, 012401.
- 498 Cenci, S. & Saavedra, S. (2019) Non-parametric estimation of the structural stability of non-
499 equilibrium community dynamics. *Nature Ecology and Evolution* **3**, 912.
- 500 Constable, G.W.A. & McKane, A.J. (2015) Models of genetic drift as limiting forms of the lotka-
501 volterra competition model. *Physical Review Letters* **114**, 038101.

- 502 Costello, E.K., Stagaman, K., Dethlefsen, L., Bohannan, B.J. & Relman, D.A. (2012) The appli-
503 cation of ecological theory toward an understanding of the human microbiome. *Science* **336**,
504 1255–1262.
- 505 Coulson, T., Kendall, B.E., Barthold, J., Plard, F., Schindler, S., Ozgul, A. & Gaillard, J.M.
506 (2017) Modeling adaptive and nonadaptive responses of populations to environmental change.
507 *The American Naturalist* **190**, 313–336.
- 508 Dakos, V., Carpenter, S.R., van Nes, E.H. & Scheffer, M. (2015) Resilience indicators: prospects
509 and limitations for early warnings of regime shifts. *Philosophical Transactions of the Royal*
510 *Society B: Biological Sciences* **370**, 20130263.
- 511 Deyle, E.R., May, R.M., Munch, S.B. & Sugihara, G. (2016) Tracking and forecasting ecosystem
512 interactions in real time. *Proceedings of the Royal Society B: Biological Sciences* **283**, 20152258.
- 513 Dobrinevski, A. & Frey, E. (2012) Extinction in neutrally stable stochastic lotka-volterra models.
514 *Physical Review E* **85**, 051903.
- 515 Domínguez-García, V., Dakos, V. & Kéfi, S. (2019) Unveiling dimensions of stability in complex
516 ecological networks. *Proceedings of the National Academy of Sciences* **116**, 25714–25720.
- 517 Donohue, I., Hillebrand, H., Montoya, J.M., Petchey, O.L., Pimm, S.L., Fowler, M.S., Healy, K.,
518 Jackson, A.L., Lurgi, M., McClean, D. *et al.* (2016) Navigating the complexity of ecological
519 stability. *Ecology Letters* **19**, 1172–1185.
- 520 Dougoud, M., Vinckenbosch, L., Rohr, R.P., Bersier, L.F. & Mazza, C. (2018) The feasibility
521 of equilibria in large ecosystems: a primary but neglected concept in the complexity-stability
522 debate. *PLOS Computational Biology* **14**, e1005988s.
- 523 Duan, J. (2015) *An Introduction to Stochastic Dynamics*. Cambridge Texts in Applied Mathe-
524 matics, Cambridge University Press, Cambridge.
- 525 Folke, C., Biggs, R., Norström, A.V., Reyers, B. & Rockström, J. (2016) Social-ecological re-
526 silience and biosphere-based sustainability science. *Ecology and Society* **21**.
- 527 Folke, C., Carpenter, S., Walker, B., Scheffer, M., Elmqvist, T., Gunderson, L. & Holling, C.S.
528 (2004) Regime shifts, resilience, and biodiversity in ecosystem management. *Annual Review of*
529 *Ecology, Evolution, and Systematics* **35**.
- 530 Friedman, J., Higgins, L.M. & Gore, J. (2017) Community structure follows simple assembly rules
531 in microbial microcosms. *Nature Ecology and Evolution* **1**, 0109.

- 532 Gibbs, H.L. & Grant, P.R. (1987) Ecological consequences of an exceptionally strong el niño event
533 on darwin's finches. *Ecology* **68**, 1735–1746.
- 534 Grilli, J., Adorisio, M., Suweis, S., Barabás, G., Banavar, J.R., Allesina, S. & Maritan, A. (2017)
535 Feasibility and coexistence of large ecological communities. *Nature Communications* **8**, 14389.
- 536 Hillebrand, H., Langenheder, S., Lebet, K., Lindström, E., Östman, Ö. & Striebel, M. (2018)
537 Decomposing multiple dimensions of stability in global change experiments. *Ecology Letters*
538 **21**, 21–30.
- 539 Hodgson, D., McDonald, J.L. & Hosken, D.J. (2015) What do you mean, 'resilient'? *Trends in*
540 *Ecology and Evolution* **30**, 503–506.
- 541 Hoek, T.A., Axelrod, K., Biancalani, T., Yurtsev, E.A., Liu, J. & Gore, J. (2016) Resource
542 availability modulates the cooperative and competitive nature of a microbial cross-feeding mu-
543 tualism. *PLoS biology* **14**, e1002540.
- 544 Hofbauer, J. & Sigmund, K. (1998) *Evolutionary Games and Population Dynamics*. Princeton
545 University Press.
- 546 Ives, A.R., Dennis, B., Cottingham, K. & Carpenter, S. (2003) Estimating community stability
547 and ecological interactions from time-series data. *Ecological Monographs* **73**, 301–330.
- 548 Justus, J. (2013) Philosophical issues in ecology. *The Philosophy of Biology*, pp. 343–371, Springer.
- 549 Kéfi, S., Domínguez-García, V., Donohue, I., Fontaine, C., Thébault, E. & Dakos, V. (2019)
550 Advancing our understanding of ecological stability. *Ecology Letters* **22**, 1349–1356.
- 551 Levin, S.A. (1998) Ecosystems and the biosphere as complex adaptive systems. *Ecosystems* **1**,
552 431–436.
- 553 Logofet, D.O. (2018) *Matrices and Graphs: Stability Problems in Mathematical Ecology*. CRC
554 Press, Boca Raton.
- 555 May, R.M. (1972) Will a large complex system be stable? *Nature* **238**, 413–414.
- 556 Medeiros, L.P., Boege, K., del Val, E., Zaldivar-Riverón, A. & Saavedra, S. (2020) Observed
557 ecological communities are formed by species combinations that are among the most likely to
558 persist under changing environments. *The American Naturalist* doi/10.1086/711663.
- 559 Murdoch, W., Briggs, C. & Nisbet, R. (2003) *Consumer-resource Dynamics*. Princeton University
560 Press, NJ.
- 561 Novak, M., Yeakel, J.D., Noble, A.E., Doak, D.F., Emmerson, M., Estes, J.A., Jacob, U., Tinker,

562 M.T. & Wootton, J.T. (2016) Characterizing species interactions to understand press perturba-
563 tions: what is the community matrix? *Annual Review of Ecology, Evolution, and Systematics*
564 **47**.

565 Pimm, S. & Lawton, J. (1977) Number of trophic levels in ecological communities. *Nature* **268**,
566 329–331.

567 Pimm, S.L., Donohue, I., Montoya, J.M. & Loreau, M. (2019) Measuring resilience is essential to
568 understand it. *Nature Sustainability* **2**, 895–897.

569 Rohr, R.P., Saavedra, S., Peralta, G., Frost, C.M., Bersier, L.F., Bascompte, J. & Tylianakis,
570 J.M. (2016) Persist or produce: a community trade-off tuned by species evenness. *The American*
571 *Naturalist* **188**, 411–422.

572 Saavedra, S., Medeiros, L.P. & AlAdwani, M. (2020) Structural forecasting of species persistence
573 under changing environments. *Ecology Letters* **23**, 1511–1521.

574 Saavedra, S., Rohr, R.P., Bascompte, J., Godoy, O., Kraft, N.J.B. & Levine, J.M. (2017) A
575 structural approach for understanding multispecies coexistence. *Ecological Monographs* **87**, 470–
576 486.

577 Smale, S. (1967) Differentiable dynamical systems. *Bull. Amer. Math. Soc.* **73**, 747–817.

578 Song, C., Ahn, S.V., Rohr, R.P. & Saavedra, S. (2020) Towards a probabilistic understanding
579 about the context-dependency of species interactions. *Trends in Ecology and Evolution* **35**,
580 384–396.

581 Song, C., Rohr, R.P. & Saavedra, S. (2018) A guideline to study the feasibility domain of multi-
582 trophic and changing ecological communities. *Journal of Theoretical Biology* **450**, 30–36.

583 Song, C. & Saavedra, S. (2018) Will a small randomly-assembled community be feasible and
584 stable. *Ecology* **99**, 743–751.

585 Song, C. & Saavedra, S. (2020) Bridging parametric and nonparametric measures of species
586 interactions unveils new insights of non-equilibrium dynamics. *BioRxiv* .

587 Steiner, C.F., Long, Z.T., Krumins, J.A. & Morin, P.J. (2006) Population and community re-
588 siliance in multitrophic communities. *Ecology* **87**, 996–1007.

589 Strogatz, S.H. (2001) *Nonlinear Dynamics and Chaos*. Westview Press.

590 Tabi, A., Pennekamp, F., Altermatt, F., Alther, R., Fronhofer, E.A., Horgan, K., Mächler, E.,
591 Pontarp, M., Petchey, O.L. & Saavedra, S. (2020) Species multidimensional effects explain

592 idiosyncratic responses of communities to environmental change. *Nature Ecology and Evolution*
593 **4**, 1036–1043.

594 Ushio, M., Hsieh, C.h., Masuda, R., Deyle, E.R., Ye, H., Chang, C.W., Sugihara, G. & Kon-
595 doh, M. (2018) Fluctuating interaction network and time-varying stability of a natural fish
596 community. *Nature* **554**, 360–363.

Accepted Article

Glossary

Asymptotic dynamical stability: The capacity of a dynamical system to return to a quantitative equilibrium reference state after a given perturbation acting on its state variables (i.e., species abundances) (Strogatz, 2001).

Dynamical indicator: A measure of resilience related to perturbations acting on species abundances.

Feasibility domain: The set of directions of parameter values (here intrinsic growth rates) compatible with positive solutions for all species (i.e., feasible system).

Full recovery: The return rate along the slowest direction following a perturbation acting on species abundances. We measure full recovery as the largest eigenvalue (λ_1) of the Jacobian matrix evaluated at an equilibrium state.

Full resilience: The capacity of a system to maintain its full species composition through the recovery and resistance of all species. Full resilience is partitioned into full recovery, which is related to abundance perturbations (i.e., asymptotic dynamical stability), and full resistance, which is related to parameter perturbations (i.e., structural stability).

Full resistance: The largest random parameter perturbation that the system can withstand before losing any species. We measure full resistance as the distance of an equilibrium state to the closest border ($\min\{d_b\}$) of the feasibility domain ($D_F(\mathbf{A})$).

Partial recovery: The return rate along the second fastest direction following a perturbation acting on species abundances. We measure partial recovery as the second smallest eigenvalue (λ_{S-1}) of the Jacobian matrix evaluated at an equilibrium state.

Partial resilience: The capacity of a system to maintain a partial species composition through the recovery and resistance of a subset of species. Partial resilience is partitioned into partial recovery, which is related to abundance perturbations (i.e., asymptotic dynamical stability), and partial resistance, which is related to parameter perturbations (i.e., structural stability).

Partial resistance: The largest random parameter perturbation that a system can withstand before at most a single species survives. We measure partial resistance as the distance of an equilibrium state to the closest vertex ($\min\{d_v\}$) of the feasibility domain ($D_F(\mathbf{A})$).

Perturbation: Any event that impacts the species abundances directly or the rules that govern population dynamics in an ecological system (i.e., the structure of the ecological system) (Justus, 2013).

Population dynamics model: A mathematical idealized description of the causal relationships (mechanistic or phenomenological) connecting the change of a population through time as a function of abiotic and biotic factors (Case, 2000).

Recovery: The rate of return (or time, if inverted) of an ecological system to a reference state after a given perturbation (Hodgson *et al.*, 2015).

Reference state: The state of an ecological system against which the perturbed system will be compared to (Justus, 2013). The reference state can be quantitative (e.g., the species abundances at equilibrium) or qualitative (e.g., the species composition of the system).

Resilience: Ability of an ecological system (i.e., set of interacting species) to resist and recover from external perturbations (Hodgson *et al.*, 2015).

Resistance: The capacity of an ecological system to resist changes in relation to its reference state after a given perturbation (Hodgson *et al.*, 2015).

Structural indicator: A measure of resilience related to perturbations acting on model parameters.

Structural stability: The capacity of a dynamical system to retain the topology of the phase portrait (i.e., the qualitative behavior of the trajectories) after a given perturbation to its structure (i.e., governing laws or model parameters) (Strogatz, 2001).

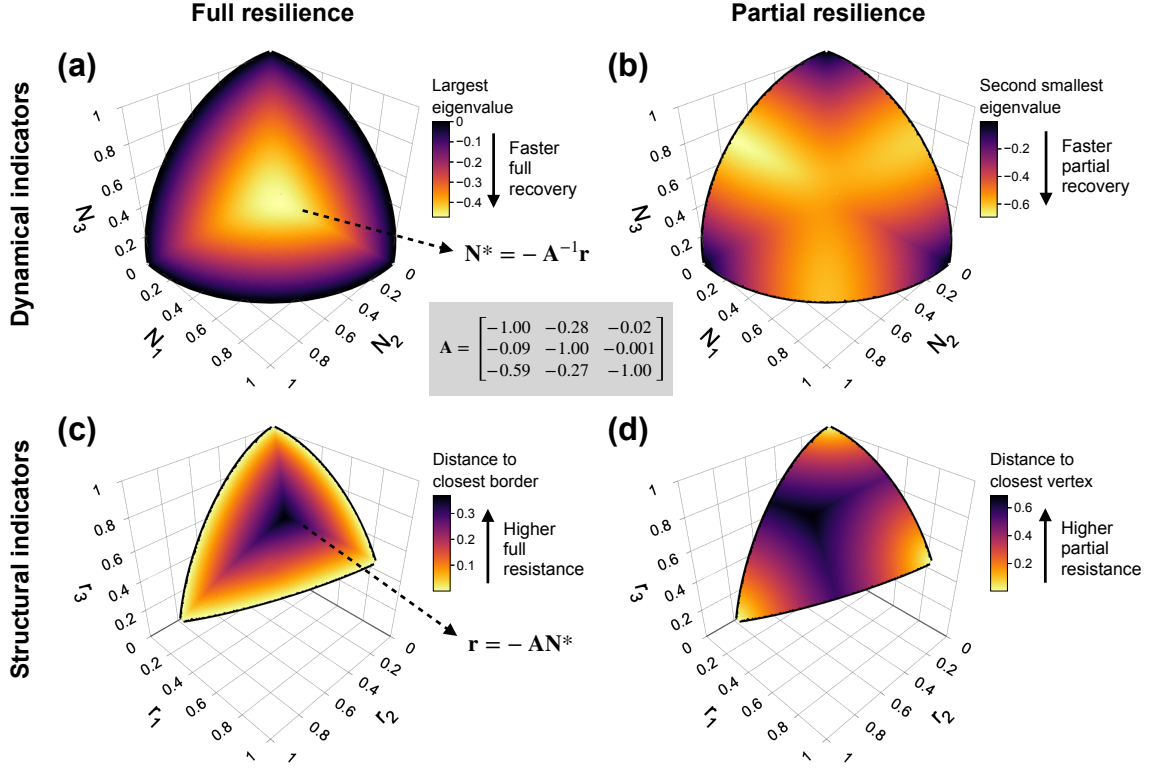


Figure 1: **Dynamical and structural indicators of full and partial resilience.** (a) An illustrative example of a 3-dimensional space of species abundances at equilibrium ($\mathbf{N}^* = [N_1^*, N_2^*, N_3^*]^\top$) colored according to the largest eigenvalue (λ_1) of the Jacobian matrix (\mathbf{J}) evaluated at equilibrium. The interaction matrix \mathbf{A} of this 3-species competition system is shown in the center of the figure. Lower values of λ_1 indicate a faster full recovery of the system after abundance perturbations. Note that this space corresponds to the positive orthant of the unit sphere (i.e., $\|\mathbf{N}^*\| = 1$, $N_i^* > 0 \forall i$). (b) The same space of species abundances, but colored according to the second smallest eigenvalue (λ_2) of \mathbf{J} evaluated at equilibrium. Lower values of λ_2 indicate a faster partial recovery after abundance perturbations. (c) The space of intrinsic growth rates ($\mathbf{r} = [r_1, r_2, r_3]^\top$) for the same system shown in (a) and (b) colored according to the distance to closest border ($\min\{d_b\}$) of the feasibility domain ($D_F(\mathbf{A})$), which are indicated as black curves. Higher values of $\min\{d_b\}$ indicate a higher full resistance to perturbations on intrinsic growth rates. Note that \mathbf{r} -vectors on the feasibility domain are normalized to unit norm (i.e., $\|\mathbf{r}\| = 1$). (d) The same space of intrinsic growth rates, but colored according to the distance to closest vertex ($\min\{d_v\}$) of $D_F(\mathbf{A})$. Higher values of $\min\{d_v\}$ indicate a higher partial resistance to perturbations on intrinsic growth rates.

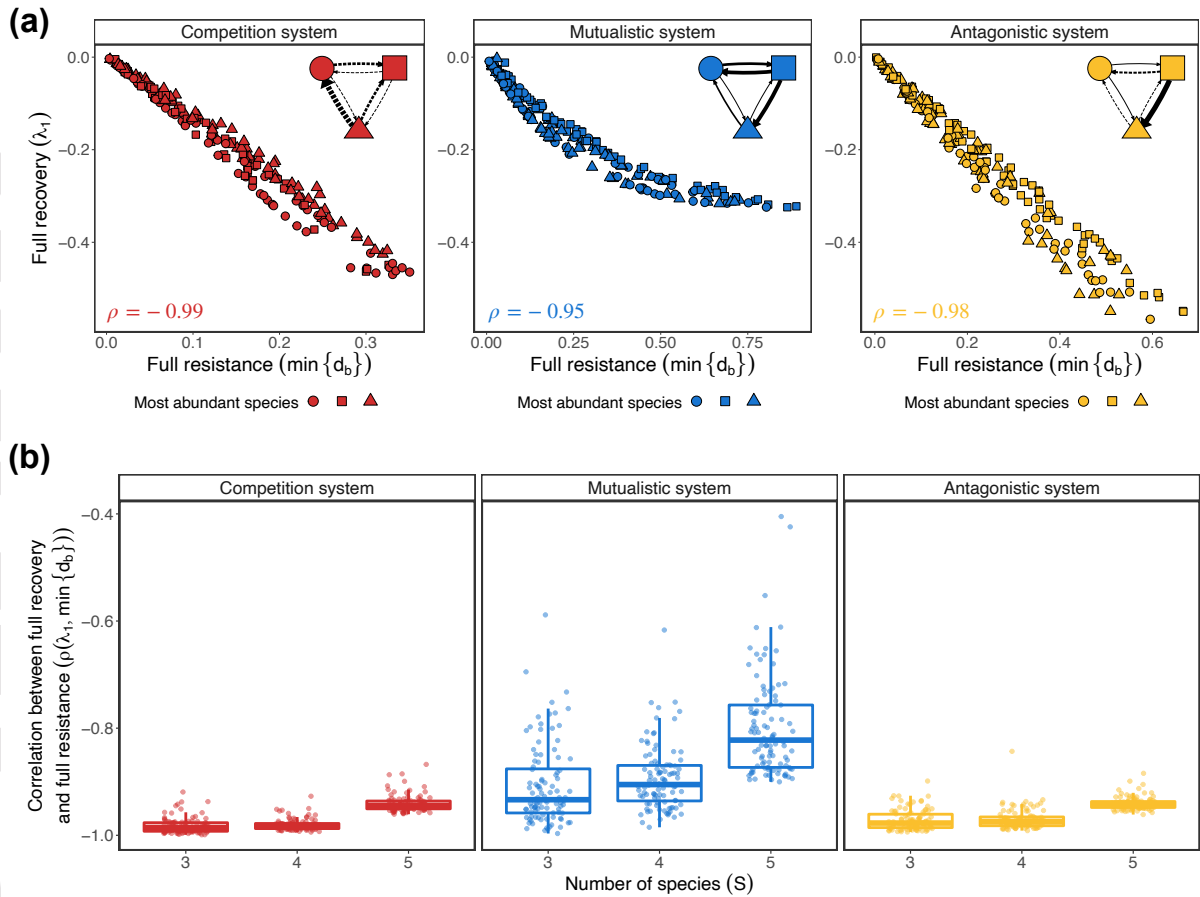


Figure 2: **Relationship between full recovery and full resistance in theoretical systems.** (a) Each panel shows 200 values of full recovery (largest eigenvalue, λ_1) and full resistance (distance to closest border, $\min\{d_b\}$) of one illustrative theoretical random system with three species (red: competition system, blue: mutualistic system, and yellow: antagonistic system). Interaction networks on the top right corner of each panel depict the interaction matrices \mathbf{A} (dashed line: negative interaction, solid line: positive interaction, and line width: interaction strength). Point shapes (circle, square, and triangle) correspond to the species with the highest abundance at that equilibrium state. Correlation values between λ_1 and $\min\{d_b\}$ are shown in the bottom left corner of each panel. The competition system is the same one as shown in Figure 1. (b) Each panel shows the correlation values between λ_1 and $\min\{d_b\}$ for a given type of system and for three system sizes ($S = 3, 4,$ and 5). Boxplots denote the median and interquartile range and points show the actual correlation values obtained for each system type and size (100 values per boxplot corresponding to 100 theoretical systems).

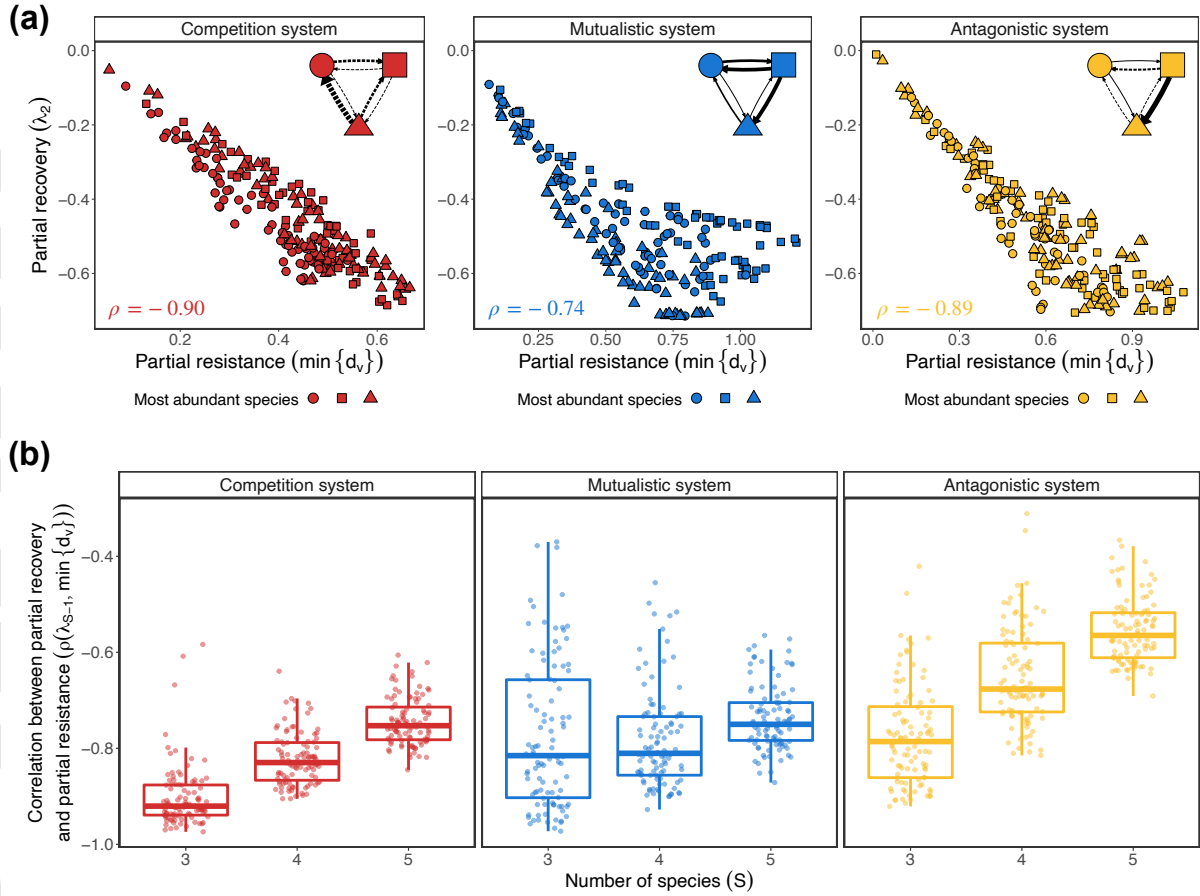


Figure 3: Relationship between partial recovery and partial resistance in theoretical systems. (a) Each panel shows 200 values of partial recovery (second smallest eigenvalue, λ_2) and partial resistance (distance to closest vertex, $\min\{d_v\}$) of the same illustrative theoretical random systems with three species shown in Figure 2a (red: competition system, blue: mutualistic system, and yellow: antagonistic system). Interaction networks on the top right corner of each panel depict the interaction matrices \mathbf{A} (dashed line: negative interaction, solid line: positive interaction, and line width: interaction strength). Point shapes (circle, square, and triangle) correspond to the species with the highest abundance at the equilibrium state. Correlation values between λ_2 and $\min\{d_v\}$ are shown in the bottom left corner of each panel. The competition system is the same one as shown in Figure 1. (b) Each panel shows the correlation values between λ_{S-1} and $\min\{d_v\}$ for a given type of system and for three system sizes ($S = 3, 4,$ and 5). Boxplots denote the median and interquartile range and points show the actual correlation values obtained for each system type and size (100 values per boxplot corresponding to the same 100 theoretical systems from Figure 2b).

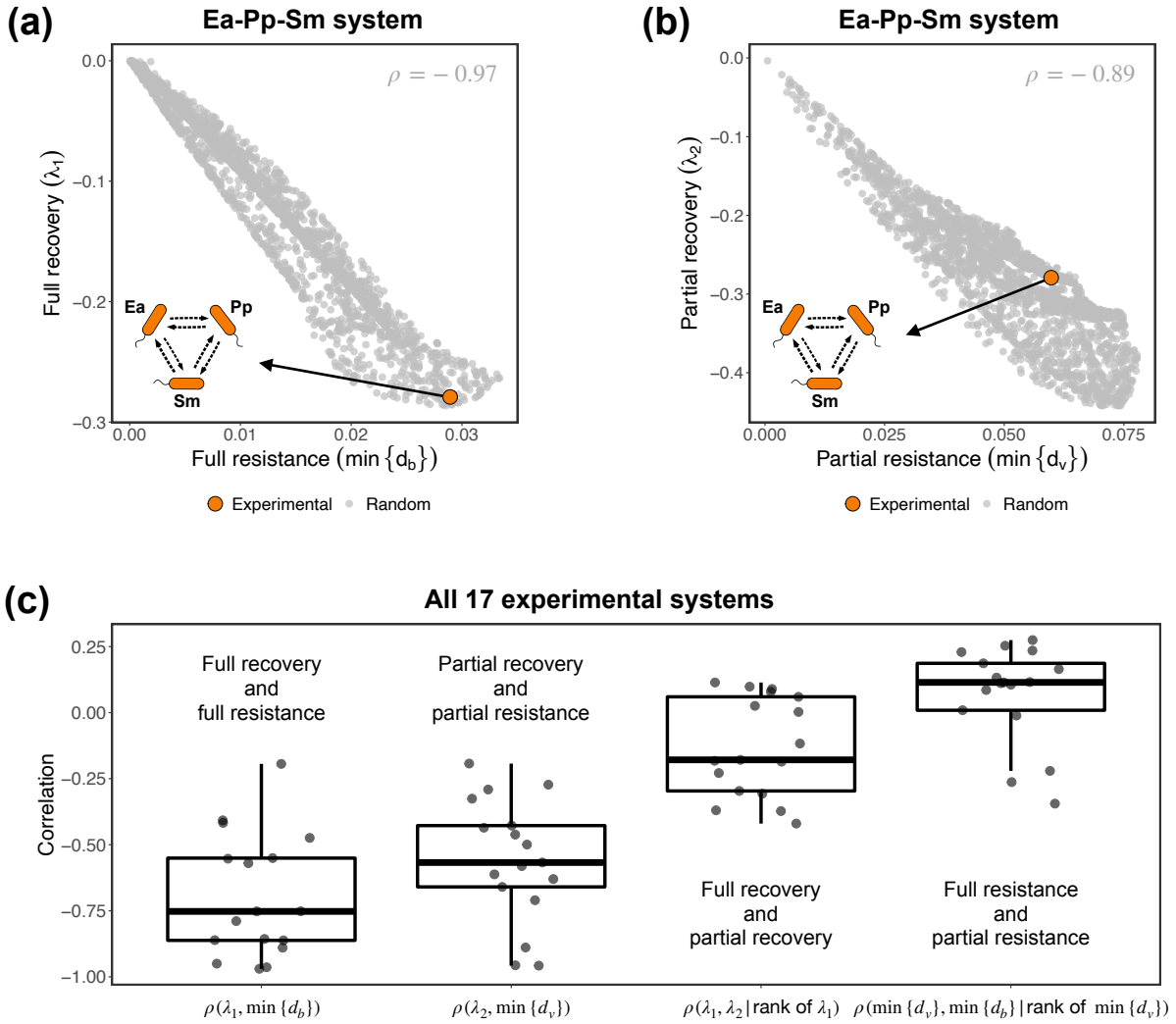


Figure 4: Relationship between recovery and resistance in experimental microbial systems. (a) Full recovery (largest eigenvalue, λ_1) and full resistance (distance to closest border, $\min\{d_b\}$) for one illustrative 3-species experimental system. Each gray point corresponds to one of 2,000 randomly sampled feasible and dynamically stable equilibrium states \mathbf{N}^* and the orange point corresponds to the λ_1 and $\min\{d_b\}$ values of the experimentally parameterized system. (b) Partial recovery (second smallest eigenvalue, λ_2) and partial resistance (distance to closest vertex, $\min\{d_v\}$) for the same experimental system shown in (a). In (a) and (b), the interaction network depicts the competition interactions between *Enterobacter aerogenes* (Ea), *Pseudomonas putida* (Pp), and *Serratia marcescens* (Sm). Correlation values computed using the gray points are shown in the top right corner of each panel. (c) Each boxplot shows a given correlation computed for all 17 experimental systems. Note that $\rho(\lambda_1, \min\{d_b\})$ and $\rho(\lambda_2, \min\{d_v\})$ are expected to be strong and negative, while $\rho(\lambda_1, \lambda_2 | \text{rank of } \lambda_1)$ and $\rho(\min\{d_v\}, \min\{d_b\} | \text{rank of } \min\{d_v\})$ are expected to be close to zero. Boxplots denote the median and interquartile range and points show the actual correlation values obtained for each system (17 values per boxplot corresponding to the 17 experimental systems).

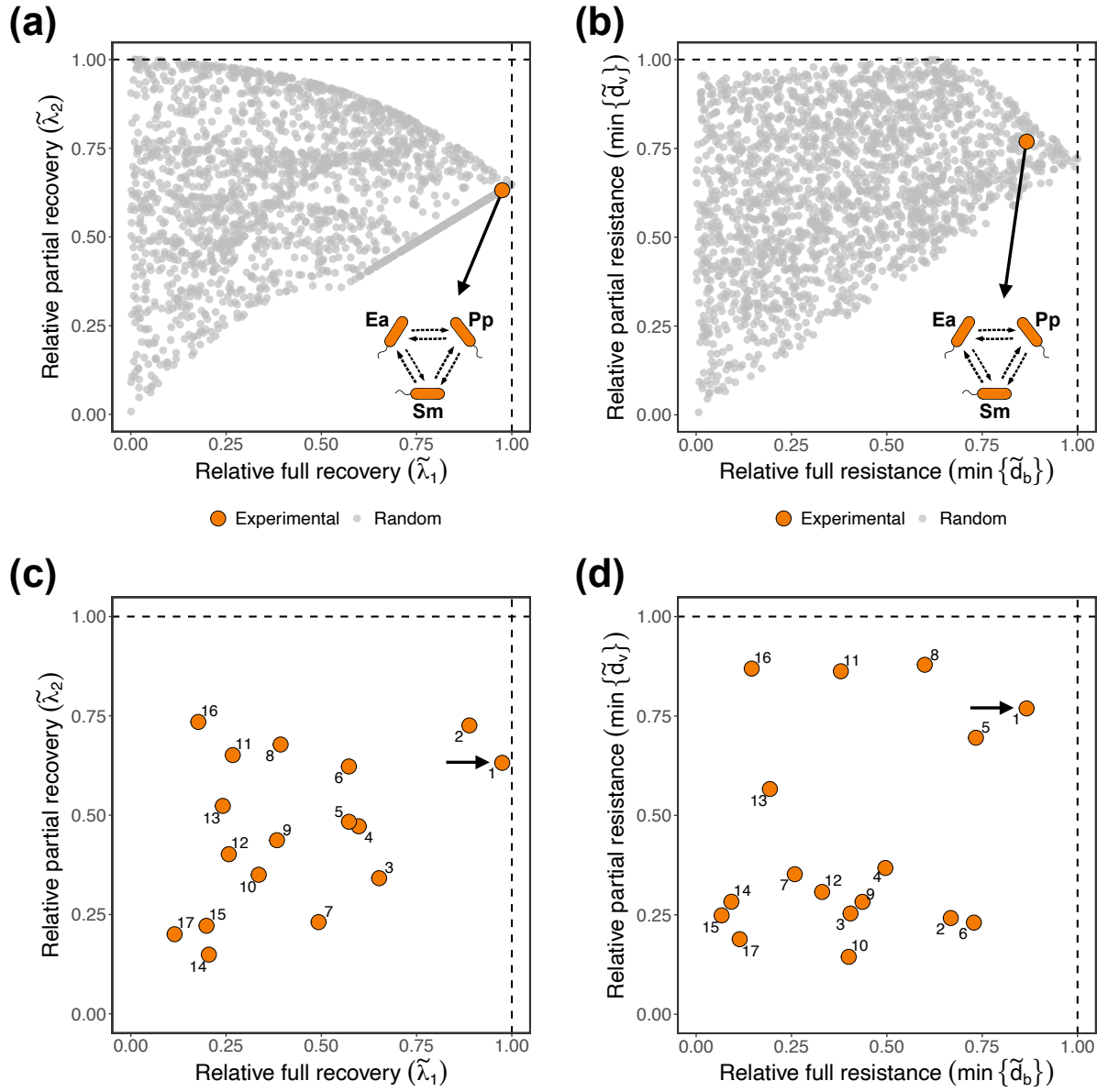


Figure 5: Complementarity between full and partial resilience in experimental microbial systems. (a) Relative full recovery ($\tilde{\lambda}_1$) and relative partial recovery ($\tilde{\lambda}_2$) for the same illustrative 3-species experimental system from Figure 4a (large orange point) as well as 2,000 values of $\tilde{\lambda}_1$ and $\tilde{\lambda}_2$ randomly sampled across the feasibility domain ($D_F(\mathbf{A})$) of this system (small gray points). (b) Relative full resistance ($\min\{\tilde{d}_b\}$) and relative partial resistance ($\min\{\tilde{d}_v\}$) for the same system shown in (a) (large orange point) as well as 2,000 values of $\min\{\tilde{d}_b\}$ and $\min\{\tilde{d}_v\}$ randomly sampled across $D_F(\mathbf{A})$ (small gray points). In (a) and (b), the interaction network depicts the competition interactions between *Enterobacter aerogenes* (Ea), *Pseudomonas putida* (Pp), and *Serratia marcescens* (Sm). Note that systems close to 1 (dashed lines) are maximizing recovery and/or resistance. (c) Relative full ($\tilde{\lambda}_1$) and partial ($\tilde{\lambda}_2$) recovery for all 17 experimentally parameterized 3-species systems. The point highlighted with an arrow represents the system depicted in (a) and labels next to points indicate the experimental systems (Table S3). (d) Relative full ($\min\{\tilde{d}_b\}$) and partial ($\min\{\tilde{d}_v\}$) resistance for the same 17 experimentally parameterized 3-species systems shown in (c). The point highlighted with an arrow represents the system depicted in (b) and labels correspond to the same systems as in (c).